

## Integrating Multi-Sensor Remote Sensing Data for Land Use/Cover Mapping in a Tropical Mountainous Area in Northern Thailand

YI-CHEN WANG\*, CHEN-CHIEH FENG and HUAN VU DUC

*Department of Geography, National University of Singapore, Block AS2 #03-01, 1 Arts Link, Singapore 117570.*

*\*Corresponding author. Email: geowyc@nus.edu.sg*

*Received 2 June 2011; Revised 2 October 2011; Accepted 23 October 2011*

### Abstract

Accurate mapping of land use/cover conditions provides essential information for managing natural resources and is critical for further examination of land use/cover change and its subsequent impacts on the environment. Remote sensing offers a means of acquiring land use/cover data in a timely manner, with optical remote sensing images commonly being used in land use/cover related studies. The persistent cloud cover during the rainy season in Southeast Asia, however, presents a challenge for using optical images in land use/cover mapping. Integrating multi-sensor images of different spectral domains is thus desirable because more information can be extracted to improve the mapping accuracy. The purpose of this study is to assess the potential of using multi-sensor data sets for land use/cover mapping in a tropical mountainous area in northern Thailand. Optical data from Landsat Thematic Mapper, radar images from Advanced Land Observing Satellite/Phased Array type L-band Synthetic Aperture Radar (PALSAR), and topographical data were used, providing complementary information on land use/cover. Classification and accuracy assessment were conducted for 12 different combinations of the data sets. The results suggested that short crop mapping using multi-temporal Phased Array type L-band Synthetic Aperture Radar images offered insights into the distributions of crop and paddy fields. Because of the mountainous environment of the study area, combining topographic data of elevation and slope into the classification greatly reduced the confusion between different land use/cover types. Improvement of classification accuracy was evident especially in separating evergreen and deciduous forests from other vegetation types and discriminating urban village and the fallow field classes.

**KEY WORDS** *land use; land cover; multi-sensor; terrain; Landsat; optical; ALOS-PALSAR; radar; remote sensing*

### ACRONYMS

|       |  |
|-------|--|
| ALOS  | Advanced Land Observing Satellite                              |
| ASTER | Advanced Spaceborne Thermal Emission and Reflection Radiometer |
| DEM   | digital elevation model  |
| MLC   | Maximum Likelihood Classifier                                  |

|        |   |
|--------|---|
| PALSAR | Phased Array type L-band Synthetic Aperture Radar |
| SAR    | Synthetic Aperture Radar                          |
| SPOT   | the Système Pour l'Observation de la Terre        |
| TM     | Thematic Mapper                                   |

## Introduction

Humid tropical forests harbor the richest terrestrial reservoir of biological diversity but suffer from rapid land use/cover change (Asner *et al.*, 2009). In particular, the region of Southeast Asia has experienced the highest percentage deforestation rate and most prominent forest degradation (Achard *et al.*, 2002; Mayaux *et al.*, 2005). Studies have suggested possible environmental impacts of land change, ranging from effects on stream water quality and land surface temperature to changes in the global carbon cycle (Foley *et al.*, 2005; Zhou and Wang, 2011). Understanding and predicting the impacts of land change are critical for sustainable management of natural resources, which often require accurate mapping of land use/cover conditions (Giri *et al.*, 2003).

Optical remotely sensed data, such as the Landsat Thematic Mapper (TM) and the Système Pour l'Observation de la Terre (SPOT) images, are multispectral, allowing most land cover types to be classified (Peng *et al.*, 2005). Temperate regions have seen great applications of optical images in land use/cover mapping (Bartalev *et al.*, 2003). Humid Southeast Asia, however, faces a haze issue and persistent cloud cover during the rainy season can last up to 6 months. This greatly limits the use of optical images in land use/cover related studies especially in tropical mountainous areas because cloud-free scenes are often unavailable.

There are at least two advantages to include radar images in land use/cover mapping of the humid tropics where the main forest conversion process has been the transformation of closed, open, or fragmented forests to agriculture (Achard *et al.*, 2002). First, radar remote sensing with microwave radiation has a strong penetration capability and is operational regardless of the frequency and volatility of cloud cover (Gao, 2009). For example, Synthetic Aperture Radar (SAR) provides cloud-free images that can be acquired in almost any weather condition. Second, for forest landscapes mixed with agricultural practices, various vegetation and crop types are often difficult to spectrally differentiate using only optical images. By combining radar and optical images, an additional portion of the spectrum is available for classification. Also,

because radar responds more to surface feature structures rather than reflectivity, radar data are potentially an advantageous addition to optical data.

Many land use/cover classification studies have reported using multi-sensor images such as optical and radar data (Aschbacher *et al.*, 1995; Haack and Bechdol, 2000; Hamilton *et al.*, 2007). Prior work has also incorporated ancillary data on terrain to improve classification accuracy in mountainous areas. For example, the addition of elevation data to SPOT images over an agricultural test site in southern France yielded an accuracy improvement of 4% (Kanellopoulos and Wilkinson, 1997). Integrating SAR data with terrain factors in southern Argentina also improved the classification accuracy of 3–26% when two of the three terrain factors (i.e. elevation, slope, and aspect) were used compared with using a single terrain factor and the radar textures; moreover, the accuracy increased by 44% by adding all three terrain factors compared with the result using radar textures alone (Peng *et al.*, 2005). Although these studies have provided fruitful results in land use/cover mapping, scant attention has been paid to the tropical mountainous forests in Southeast Asia, where land change has been occurring at an unprecedented rate and the probable environmental consequences are of particular concern (Thanapakpawin *et al.*, 2006).

The purpose of this study was to assess the potential of using multi-sensor data with terrain information for land use/cover mapping of tropical mountainous areas in Southeast Asia. The data sets used consisted of optical data from Landsat TM, radar images from the Phased Array type L-band Synthesis Aperture Radar (PALSAR) on the Advanced Land Observing Satellite (ALOS), and terrain information in the form of a Digital Elevation Model (DEM) derived from the Advanced Spaceborne Thermal Emission and Reflection Radiometer (ASTER) for an area in northern Thailand. The study hypothesised that a combination of these data sets would allow agricultural land use types to be extracted and evergreen and deciduous forests to be separated from other vegetation types. The analyses carried out included analysing multi-temporal PALSAR data to identify agricultural

land use types with short crop rotation; integrating optical data, radar images, and topographical data for land use/cover classification; and evaluating the classification accuracy. The aim of the study was to determine whether the combination of multi-sensor data sets can improve land use/cover classification in tropical mountainous areas in terms of classification accuracy.

### Study area

The study area is located in the Chiang Mai Province in northern Thailand (Figure 1). The spatial extent of analysis is the coverage of one ALOS-PALSAR scene, approximately 70 km × 70 km (18°41′59.69″ N to 19°21′31.88″ N and 98°38′10.58″ E to 99°24′52.92″ E). It has a mountainous terrain with elevation ranging from about 300 to 1800 m above sea level; 52% and 15% of the area are below 600 m and above 1000 m, respectively. The area includes six districts of the Chiang Mai province (Figure 1) and covers the Mae Rim and the Mae Ping Part II catchments of the Ping River basin, which has

experienced rapid forest conversion into agricultural crops in the last several decades (Giri *et al.*, 2003; Thomas, 2006). The area is characterised by a tropical monsoon climate with a rainy season occurring from May to October. Annual mean rainfall ranges between 1100 and 1300 mm, of which 80% falls within the 6-month rainy season (Gardner *et al.*, 2007). Annual mean temperature of northern Thailand is 26.1°C (Thai Meteorological Department, 2010).

Crop rotation is common in the study area with rice in the rainy season and soybean, shallot, tomato, and onion in the dry season. According to local farming practice, short crops, such as maize and sweet corn, are grown from April to early September, and paddy rice is grown from May to October. Land is increasingly being converted for fruit tree production, such as longan, lychee, and oranges, because of good profitability (Ekasingh *et al.*, 2005). Private business for resorts and recreation centres is also notable as a result of its proximity to a major tourist destination, the city of Chiang Mai. Natural forests and

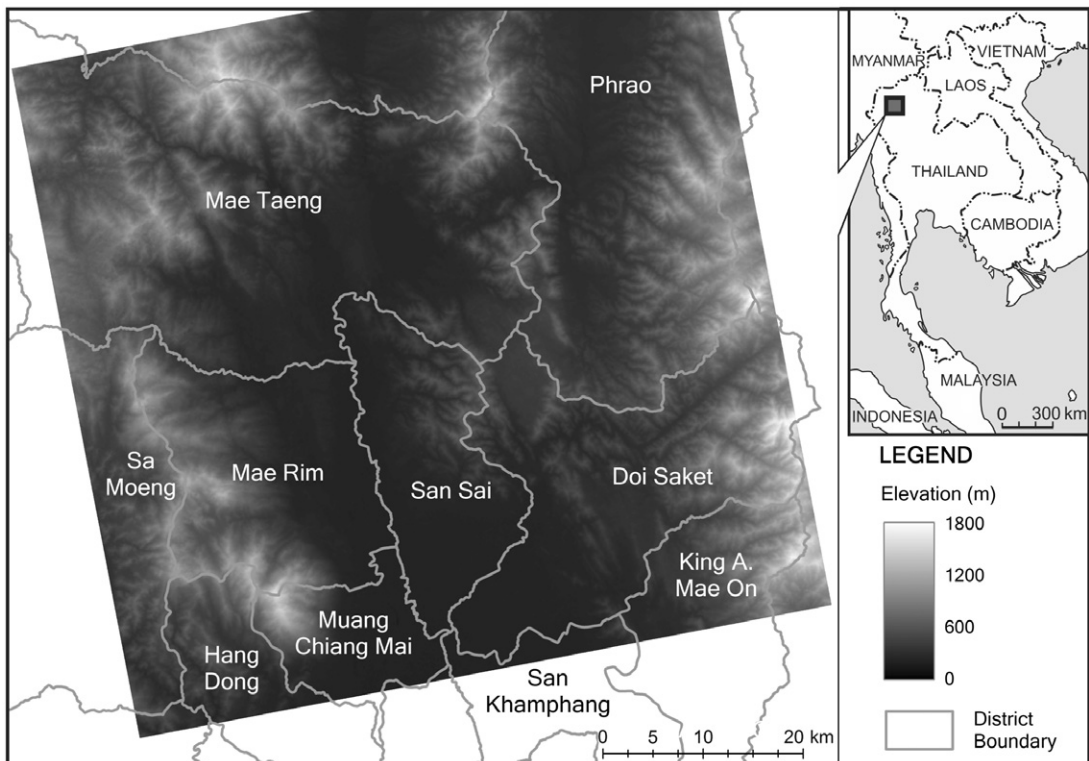


Figure 1 Location of the study area in northern Thailand. The spatial extent of the study area is one Advanced Land Observing Satellite/Phased Array type L-band Synthetic Aperture Radar scene, covering 70 km × 70 km and six districts of the Chiang Mai province.

ecological conditions exhibit altitudinal zones in northern Thailand, and altitudes of 600 and 1000 m have been used to distinguish lowland, midland, and highland zones in the Ping River Basin (Thomas, 2006). The natural forests of the lowland, midland, and highland zones are respectively dry dipterocarp forests, mixed deciduous forests, and hill evergreen and coniferous forests with small areas above 1800 m being moist temperate forests. Current land use patterns, albeit influenced by a variety of government policies and socio-economic factors, remain closely related to the altitudinal zones (Thomas *et al.*, 2004).

## Materials and methods

### Data

Data used for land use/cover classification in this study included remote sensing images and terrain information. The remote sensing images consisted of one optical Landsat TM image and two radar ALOS-PALSAR images. The Landsat TM scene dated 2 April 2007 in the dry season had a spatial resolution of 30 m for all of its spectral bands, except for the thermal band, for which the resolution is 120 m. All the bands, except for the thermal band, were included in the analysis. The ALOS PALSAR, which acquires L-band at 23.6 cm, has two modes of polarisation as HH (horizontally transmitted and horizontally received) and HV (horizontally transmitted and

vertically received). The two PALSAR images with a 12.5 m spatial resolution and 38.7° incident angle were taken in the rainy season on 11 June 2007 and 11 September 2007. The Earth Remote Sensing Data Analysis Center (ERSDAC) has ortho-rectified the PALSAR data to higher level product format (Level 4.1) in Universal Transverse Mercator (Zone 47) World Geodetic System 1984 datum, and radiometric calibrated and extracted radar backscattering in Beta Nought (ERSDAC, 2009a). The ALOS PALSAR attains geometric and radiometric accuracy at 9.3 m and 0.2 dB, respectively (Japan Aerospace Exploration Agency, 2007).

Terrain information was derived from the ASTER DEM, a 1 arc-second (approximately 30 m) grid. The estimated accuracies were 20 m for vertical data and 30 m for horizontal data at 95 % confidence (ERSDAC, 2009b). The 1:50 000 topographical maps prepared by the Royal Thai Survey Department (RTSD) in 1999 were used to extract Geographic Information System (GIS) data such as road networks and administration boundaries. The land use/cover mapping procedure is shown in Figure 2. Details are provided below for the steps of geometric correction, speckle noise reduction, short crop mapping, multi-sensor data classification, post-classification editing, and accuracy assessment to produce the final land use/cover map. Software used in data processing and analysis included ERDAS Imagine 9.1 (Leica Geosystems

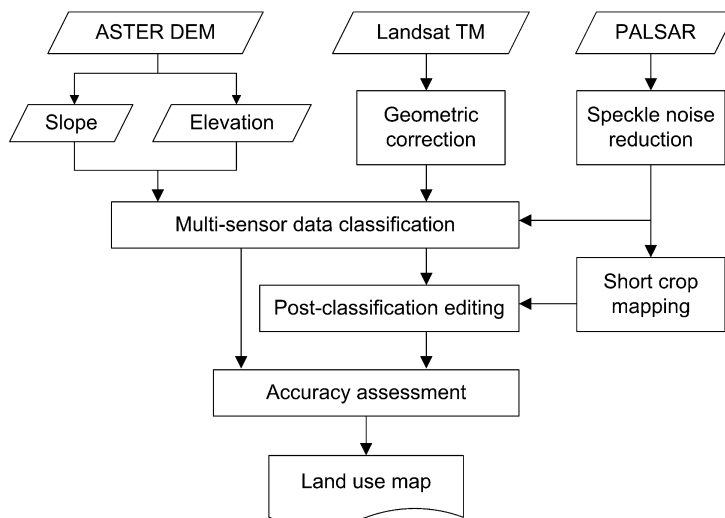


Figure 2 Procedure of integrating multi-sensor remote sensing data for land use/cover mapping. ASTER, Advanced Spaceborne Thermal Emission and Reflection Radiometer; DEM, digital elevation model; TM, Thematic Mapper; PALSAR, Phased Array type L-band Synthetic Aperture Radar.

Geospatial Imaging, Norcross, GA, USA), ENVI 4.6 (Exelis VIS, Boulder, CO, USA), and ArcGIS 9.3 (ESRI, Redlands, CA, USA).

#### Geometric correction

The GIS road network data layer derived from the RTSD topographic maps was calibrated using Global Positioning System (GPS) data to achieve a high accuracy for geometric correction of the Landsat TM image required for multi-sensor data integration. GPS data were collected along the road networks throughout the study area in February 2009 using the HP iPAQ Bluetooth GPS Navigation System (Hewlett-Packard, Houston, TX, USA). The horizontal position error of the GPS was less than 15 m according to the maximum estimated position error indicated by the GPS unit. A total of 12 GPS points, including road intersections, bridges, and building and reservoir corners, were selected as ground control points for geometric correction because they could be identified and located accurately on the image. The final root mean square error was 30 m.

#### Speckle noise reduction for PALSAR images

Speckle is a granular noise that appears in a seemingly random pattern of brighter and darker pixels in radar images (Lillesand and Kiefer, 1999). The presence of speckle in radar images makes the radiometric and textural information less efficient for distinguishing land use/cover types. Reduction of speckle noise is thus important to increase the image quality for discrimination of different land use/cover types (Gao, 2009). The Gamma Maximum-A-Posteriori (MAP) filter removes distinctive pixels in homogeneous areas and retains edge sharpness, thereby enhancing the scene targets, which is useful for land use/cover classification of forest and agricultural areas (Baraldi and Parmiggiani, 1995). The Gamma MAP filter with a kernel size of  $3 \times 3$  pixels was thus performed on the PALSAR images for the homogeneous areas to better preserve texture information.

#### Short crop mapping

Forest conversion to agricultural land has been an important cause of deforestation in northern Thailand highlands (Giri *et al.*, 2003). The common agricultural land use types in northern Thailand are shifting cultivation and short crop rotation (Thomas *et al.*, 2004; Ekasingh *et al.*, 2005). Time-series satellite images have been used to improve classification accuracy (Ver-

besselt *et al.*, 2010); images of different times of a year may thus help to identify agricultural land use types with short crop rotation. For example, open water in the early rice growing stage in paddy fields in April and May can seriously affect the reflectance of infrared wavelengths, resulting in paddy field being classified as a water body if the April 2007 Landsat image is used on its own. Similarly, crop fields, such as maize and sweet corn grown from April to September, may be misinterpreted as bare land or fallow field when using the dry season Landsat image alone.

Radar images provide information on agricultural land use during the rainy season when optical data are often unavailable. The two PALSAR images in June and September 2007 were therefore used for short crop mapping, particularly in extracting areas of paddy and crop fields. Because of the precise radiation calibration of radar images, image ratioing was employed to identify change areas of short crop cultivation with the 11 June 2007 PALSAR image as time 1 ( $t1$ ) and the 11 September 2007 PALSAR image as time 2 ( $t2$ ). Digital number (DN) values of the two images were then used in the following equation:

$$G(i, j) = \frac{(G(i, j)_{t_1}^{HH} + G(i, j)_{t_1}^{HV}) \times 0.5}{(G(i, j)_{t_2}^{HH} + G(i, j)_{t_2}^{HV}) \times 0.5} \quad (1)$$

where  $G(i, j)$  = Ratio of DN values among the input channels at location  $(i, j)$ ,  $G(i, j)_{t_1}^{HH}$  = DN value in HH polarisation at the same location at  $t1$ ,  $G(i, j)_{t_1}^{HV}$  = DN value in HV polarisation at the same location at  $t1$ ,  $G(i, j)_{t_2}^{HH}$  = DN value in HH polarisation at the same location at  $t2$ ,  $G(i, j)_{t_2}^{HV}$  = DN value in HV polarisation at the same location at  $t2$ .

Although areas that have not changed in the interim should theoretically receive a ratio value of 1 in the divided image while all the change pixels should have a value of non 1, a threshold is recommended to distinguish pixels of change from pixels of no change (Gao, 2009). A histogram of the resulting DN ratio values was plotted; based on the range of radiometric accuracy and visual interpretation, the threshold for no change was set for ratios between 0.8 and 1.2. For pixels with ratios outside the range of 0.8–1.2, they were identified as areas of change as a result of rice ripening or crop harvesting, with ratios between 0 and 0.8 as paddy field and between 1.2 and 1.9 as crop field. The accuracy



of short crop mapping was verified using a high resolution (0.6 m) 2006 Quickbird image. Additional field verification was conducted in February and June 2009 for areas that could be accessed. The areas extracted from short crop mapping were subsequently incorporated with multi-sensor data classifications through post-classification editing in the next section.

#### *Multi-sensor data classification and post-classification editing*

Based on a land use/cover classification scheme for remotely sensed data (Anderson *et al.*, 1976), prior land use projects and studies (Thomas *et al.*, 2004; Ekasingh *et al.*, 2005; Thomas, 2006), the report of the Office of Agricultural Economy of Thailand (Office of Agricultural Economics, 2007), and field observations, a total of 14 land use/cover types were mapped in this study. These included: 1. Evergreen forest, 2. Fallow field, 3. Deciduous forest, 4. Horticultural land, 5. Orchard, 6. Forest plantation, 7. Crop field, 8. Urban village, 9. Water, 10. Range land, 11. Paddy field, 12. Barren land, 13. Pasture, and 14. Wetland. The sequence of the listed land use/cover types, from evergreen forest to paddy field, was in general distributed from high to low altitudes.

The multi-sensor data used consisted of nine input bands: one band of the PALSAR image acquired on 11 June 2007; six bands of the Landsat TM image; and one band of elevation and one band of slope, both derived from the ASTER DEM. These data were co-registered and resampled into the same pixel size of 25 m. Land use/cover classification was done using the Maximum Likelihood Classifier (MLC). Care was taken to ensure the representativeness of training samples because of their potential influence on the classification result. The more extensively a land cover was distributed over the scene, the more pixels were selected as the training samples for that class. For a class of a subordinate areal extent, Gao (2009) suggested a total training sample size of 100 pixels. In this study, the average training sample size for the land use classes was 12 197 pixels, with the maximum of 25 779 pixels for deciduous forest and the minimum of 681 pixels for barren land, all of which were considered sufficient for the MLC method according to Mather (2004). The training samples for each of the land use/cover types were determined based on local area knowledge of the research team, image interpretation, and field survey in February and June 2009.

The MLC was conducted using the same training sample set for each individual band and various combinations of bands of the multi-sensor data sets, consisting of the PALSAR image, the Landsat image, and terrain information on elevation and slope derived from the ASTER DEM. Post-classification editing was then carried out to incorporate the classifications from the multi-sensor data sets with the short crop areas extracted from short crop mapping of the multi-temporal PALSAR images. As a result, a total of 12 different combinations were produced for subsequent accuracy assessments, including: 1. PALSAR (P), 2. PALSAR-elevation (PE), 3. PALSAR-elevation-slope (PES), 4. PALSAR-elevation-slope-short crop (PES-SC), 5. Landsat TM (L), 6. Landsat TM-elevation (LE), 7. Landsat TM-elevation-slope (LES), 8. Landsat TM-elevation-slope-short crop (LES-SC), 9. Landsat TM-PALSAR (LP), 10. Landsat TM-PALSAR-elevation (LPE), 11. Landsat TM-PALSAR-elevation-slope (LPES), and 12. Landsat TM-PALSAR-elevation-slope-short crop (LPES-SC).

#### *Accuracy assessment*

To assess the classification accuracy, an aligned systematic sampling approach, modified from Ismail and Jusoff (2008), was applied. By using a grid of 4 km × 4 km (Figure 3), a total of 292 ground reference points were generated for the whole study area.

Of the 292 ground reference points, visual interpretation following Lung and Schaab (2010) was carried out for 238 points using the original Landsat image facilitated by the high resolution

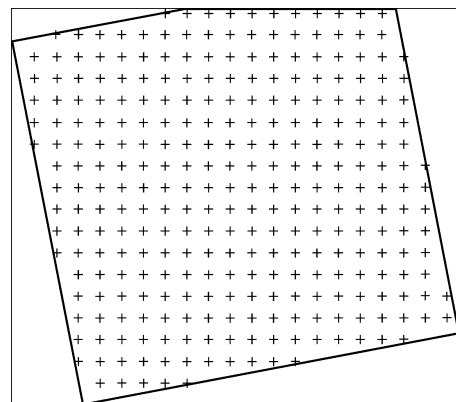


Figure 3 Distribution of the 292 reference points for classification accuracy assessment.

2006 Quickbird image, and field verification was done in late 2009 and early 2010 for 54 points where the locations could be reached. This reference data set was used in classification accuracy assessment for the 12 combinations of the multi-sensor data sets. Accuracy reports were then generated from a confusion matrix for overall accuracy, the Kappa coefficient, the producer's accuracy, and the user's accuracy. Furthermore, to examine the extent to which the multi-sensor classification was able to map the crop and paddy fields, the areas detected using short crop mapping were overlaid with the multi-sensor classification that had the best classification accuracy before the incorporation of short crop mapping.

### Results and discussion

For each of the 12 different combinations of the multi-sensor data sets, classification accuracy was assessed by referencing to the 292 referenced points distributed over the study area (cf. Figure 3). In general, the classification accuracies increased when topographic data of elevation and slope and the results of short crop mapping were combined with the remote sensing images. The overall accuracies ranged from 19.2% for using the PALSAR image alone to 89.7% for combining the Landsat and PALSAR images with elevation, slope, and short crop mapping (Table 1).

The use of the single PALSAR image (11 June 2007) produced very poor classification result, probably due to the layover and foreshortening effects on radar images caused by the terrain features in the study area. The Kappa coefficient was only 0.10. Although the smooth surface and dark tones of water and bright tones of forest plantation led to relatively high classification accuracies, low accuracies in other land use/cover types suggested the difficulty of using the tonal information of single PALSAR image in classification (Table 1). Indeed, mountainous terrains often caused distortion of radar tones, resulting in some land use/cover classes having similar brightness, such as evergreen forest (distributed in highlands) and range land (mostly found in lowlands). When elevation data were integrated with PALSAR to separate the distributions of the land use classes, the accuracies improved, which was evident from the increased producer's accuracy from 37.5% with P to 75% with PE for the evergreen forest class (Table 1). In the study area, the distribution of land use/cover is not only affected by elevation, but also

by slope. For example, deciduous forests are distributed in relatively steep areas with an average slope of about 15%, while the land use/cover type urban village is mainly located on flat ground. Thus, when slope data were further combined with elevation and the PALSAR image (i.e. PES), the accuracies for some classes improved, as seen in the increased producer's accuracy from 54.3% to 64.3% for deciduous forest and from 7.7% to 38.5% for urban village (Table 1).

Analyses involving the Landsat TM image generally produced higher accuracies than those with only the PALSAR image because the multi-spectral channels of Landsat TM enabled the differentiation of more land use/cover types. This is exhibited in the results for fallow field and barren land that 0% accuracies were produced with the use of PALSAR image (i.e. P) even when additional terrain information was incorporated (i.e. PE and PES). Conversely, the producer's accuracies for fallow field and barren land improved to 50% and 100%, respectively when the Landsat image was used (Table 1). In addition, the results in overall accuracy and Kappa coefficient were considerably improved when topographic data of elevation and slope were incorporated (i.e. LE and LES). Fallow field, deciduous forest, forest plantation, and paddy field all had relatively low accuracies when classifications were done using remote sensing images only (i.e. L and LP). The incorporation of the elevation data, however, increased the producer's accuracy from 50% with L to 71.4% with LE for fallow field. Accuracies for deciduous forest also increased when the classification was done with LPE as opposed to LP (Table 1). Indeed, land use/cover patterns in the mountainous study area remain closely related to the altitudinal zones (Thomas *et al.*, 2004), and the distribution of forest classes is closely related to elevation. Alternatively, slope plays a role in further discriminating land use/cover classes that are distributed within a similar elevation range, especially in separating deciduous forest from other vegetation types for the areas below 1000 m. Compared with using only LE, the Kappa coefficients increased from 0.69 to 0.77 when slope was included in the multi-sensor data sets (i.e. LES). The producer's accuracies also increased for deciduous forest (from 85.7% to 95.7%) and horticultural land (from 44.4% to 66.7%) from LPE to LPES (Table 1). These results underscored the usefulness of incorporating terrain information into land use/cover classification in mountainous environments. Combining terrain factors of elevation

Table 1 Accuracy assessment of the multi-sensor classifications.

| Multi-sensor data  | P     |      | PE    |      | PES   |       | PES-SC |       | L     |       | LE    |       | LES   |       | LES-SC |       | LP    |       | LPE   |       | LPES  |       | LPES-SC |       |
|--------------------|-------|------|-------|------|-------|-------|--------|-------|-------|-------|-------|-------|-------|-------|--------|-------|-------|-------|-------|-------|-------|-------|---------|-------|
|                    | PA    | UA   | PA    | UA   | PA    | UA    | PA     | UA    | PA    | UA    | PA    | UA    | PA    | UA    | PA     | UA    | PA    | UA    | PA    | UA    | PA    | UA    | PA      | UA    |
| Overall accuracy   | 19.2  |      | 43.5  |      | 50.3  |       | 52.7   |       | 55.5  |       | 73.0  |       | 80.1  |       | 81.9   |       | 55.5  |       | 74.7  |       | 87.7  |       | 89.7    |       |
| Kappa              | 0.10  |      | 0.35  |      | 0.43  |       | 0.46   |       | 0.48  |       | 0.69  |       | 0.77  |       | 0.79   |       | 0.48  |       | 0.71  |       | 0.86  |       | 0.88    |       |
| Land use class     | PA    | UA   | PA    | UA   | PA    | UA    | PA     | UA    | PA    | UA    | PA    | UA    | PA    | UA    | PA     | UA    | PA    | UA    | PA    | UA    | PA    | UA    | PA      | UA    |
| Evergreen forest   | 37.5  | 24.3 | 75.0  | 73.5 | 72.9  | 77.8  | 72.9   | 79.6  | 83.3  | 74.1  | 91.7  | 84.6  | 97.9  | 94.0  | 97.9   | 95.9  | 83.3  | 78.4  | 91.7  | 89.8  | 100.0 | 98.0  | 100.0   | 100.0 |
| Fallow field       | 0.0   | 0.0  | 0.0   | 0.0  | 0.0   | 0.0   | 0.0    | 0.0   | 50.0  | 41.2  | 71.4  | 45.5  | 92.9  | 72.2  | 92.9   | 72.2  | 42.9  | 33.3  | 71.4  | 45.5  | 100.0 | 82.4  | 100.0   | 82.4  |
| Deciduous forest   | 12.9  | 45.0 | 54.3  | 67.9 | 64.3  | 71.4  | 62.9   | 73.3  | 70.0  | 65.3  | 84.3  | 85.5  | 92.9  | 87.8  | 91.4   | 90.1  | 71.4  | 66.7  | 85.7  | 87.0  | 95.7  | 90.5  | 94.3    | 93.0  |
| Horticultural land | 22.2  | 22.2 | 44.4  | 25.0 | 44.4  | 33.3  | 44.4   | 40.0  | 44.4  | 28.6  | 22.2  | 33.3  | 22.2  | 33.3  | 22.2   | 40.0  | 55.6  | 35.7  | 44.4  | 44.4  | 66.7  | 75.0  | 66.7    | 100.0 |
| Orchard            | 11.8  | 6.9  | 11.8  | 8.0  | 29.4  | 22.7  | 29.4   | 22.7  | 29.4  | 55.6  | 35.3  | 54.6  | 64.7  | 64.7  | 64.7   | 68.8  | 29.4  | 35.7  | 52.9  | 60.0  | 82.4  | 87.5  | 88.2    | 93.3  |
| Forest             | 37.3  | 35.2 | 54.9  | 57.1 | 56.9  | 65.9  | 54.9   | 65.1  | 52.9  | 62.8  | 82.4  | 84.0  | 82.4  | 87.5  | 80.4   | 91.1  | 52.9  | 62.8  | 84.3  | 89.6  | 86.3  | 95.7  | 84.3    | 97.7  |
| Plantation         |       |      |       |      |       |       |        |       |       |       |       |       |       |       |        |       |       |       |       |       |       |       |         |       |
| Crop field         | 0.0   | 0.0  | 20.0  | 22.7 | 24.0  | 40.0  | 52.0   | 48.2  | 40.0  | 47.6  | 52.0  | 56.5  | 56.0  | 82.4  | 84.0   | 72.4  | 40.0  | 58.8  | 52.0  | 59.1  | 72.0  | 94.7  | 96.0    | 83.3  |
| Urban village      | 7.7   | 33.3 | 7.7   | 50.0 | 38.5  | 29.4  | 38.5   | 29.4  | 46.2  | 37.5  | 53.9  | 63.6  | 61.5  | 61.5  | 61.5   | 61.5  | 46.2  | 35.3  | 46.2  | 50.0  | 84.6  | 61.1  | 84.6    | 61.1  |
| Water              | 100.0 | 10.0 | 100.0 | 20.0 | 100.0 | 12.5  | 100.0  | 14.3  | 100.0 | 100.0 | 100.0 | 100.0 | 100.0 | 100.0 | 100.0  | 100.0 | 100.0 | 100.0 | 100.0 | 100.0 | 100.0 | 100.0 | 100.0   | 100.0 |
| Range land         | 0.0   | 0.0  | 22.2  | 40.0 | 66.7  | 50.0  | 66.7   | 54.6  | 11.1  | 20.0  | 44.4  | 66.7  | 77.8  | 77.8  | 77.8   | 77.8  | 22.2  | 28.6  | 33.3  | 50.0  | 88.9  | 100.0 | 88.9    | 100.0 |
| Paddy field        | 21.1  | 22.2 | 21.1  | 23.5 | 26.3  | 41.7  | 42.1   | 53.3  | 42.1  | 40.0  | 63.2  | 80.0  | 52.6  | 90.9  | 63.2   | 85.7  | 36.8  | 38.9  | 63.2  | 85.7  | 57.9  | 91.7  | 73.7    | 87.5  |
| Barren land        | 0.0   | 0.0  | 0.0   | 0.0  | 0.0   | 0.0   | 0.0    | 0.0   | 100.0 | 100.0 | 100.0 | 50.0  | 100.0 | 50.0  | 0.0    | 0.0   | 100.0 | 100.0 | 100.0 | 50.0  | 100.0 | 50.0  | 0.0     | 0.0   |
| Pasture            | 0.0   | 0.0  | 25.0  | 33.3 | 25.0  | 100.0 | 16.7   | 100.0 | 8.3   | 14.3  | 83.3  | 52.6  | 91.7  | 61.1  | 83.3   | 66.7  | 8.3   | 14.3  | 83.3  | 52.6  | 83.3  | 66.7  | 75.0    | 75.0  |
| Wetland            | 0.0   | 0.0  | 100.0 | 18.8 | 100.0 | 13.6  | 100.0  | 16.7  | 66.7  | 22.2  | 66.7  | 40.0  | 66.7  | 25.0  | 66.7   | 33.3  | 33.3  | 11.1  | 66.7  | 50.0  | 100.0 | 42.9  | 100.0   | 60.0  |

Note: All measurements except Kappa are in percentage.  
P, PALSAR image; L, Landsat TM image; E, elevation; S, slope; SC, short crop mapping from the multi-temporal PALSAR images; PA, producer's accuracy; UA, user's accuracy.



and slope greatly reduced confusion between different land use/cover types, thereby improving the measures of classification accuracy.

Among the nine combinations of multi-sensor data sets before integrating with short crop mapping, LPES had the best overall accuracy and the highest producer's and user's accuracies for the land use classes of crop field and paddy field (Table 1). The distributions of crop and paddy fields detected by short crop mapping were therefore overlaid with the classification result of LPES to examine the extent to which the LPES classification was able to map these two land use classes. Short crop mapping using multi-temporal PALSAR images detected that 6.1% (285.7 km<sup>2</sup>) and 1.8% (81.7 km<sup>2</sup>) of the study area were crop and paddy fields, respectively. Among the areas of crop field and paddy field detected by short crop mapping, LPES classified some of the crop areas into deciduous forest (20.6%) and paddy field (13.6%), and some of the paddies into crop field (19.9%) and pasture (14.4%) (Table 2). The results showed the deficiencies of the LPES classification in mapping the short crop land use classes.

The accuracies for short crop agricultural land use classes were improved when the results of short crop mapping were integrated with the multi-sensor data sets. As demonstrated in the addition of short crop mapping to PES (i.e. PES-

SC), the producer's accuracy for crop field increased from 24% to 52% and for paddy field from 26.3% to 42.1% (Table 1). For the multi-sensor classifications of LPES compared with LPES-SC, the producer's accuracies for crop field and paddy field notably improved from 72% to 96% and from 57.9% to 73.7%, respectively. The results echoed prior studies (e.g. Pan *et al.*, 2010) that the accuracy of mapping crop fields could be improved by including multi-temporal data in the procedure. The capability of radar to penetrate clouds and the sensitivity of its signal to the surface roughness provided information on agricultural land use during the rainy season. In the 11 June 2007 PALSAR image, young rice paddies appeared in dark tone because most of the paddy fields were still covered by water, while short crops in the middle of their growth stage appeared in bright tones. Conversely, in the 11 September 2007 image, ripened rice paddies appeared in bright tones, while harvested short crop fields that had become fallow fields appeared in dark tone. Short crop mapping from the multi-temporal PALSAR images could therefore be of great benefit in discriminating agricultural land use types, particularly in tropical mountainous areas with persistent cloud cover during the rainy season.

The best classification result was produced when short crop mapping and elevation and slope

Table 2 Composition of the land use/cover types derived using the multi-sensor Landsat-PALSAR-elevation-slope (LPES) classification for the areas of crop and paddy fields extracted using the short crop mapping of the multi-temporal PALSAR data.

| Land use/cover types<br>classified using the LPES | Short crop mapping of the multi-temporal PALSAR data |       |                         |       |
|---|--|-------|-------------------------|-------|
|   | Crop field   |       | Paddy field             |       |
|   | Area (km <sup>2</sup> )                              | %     | Area (km <sup>2</sup> ) | %     |
| Evergreen forest                                  | 31.2   | 10.9  | 1.3                     | 1.6   |
| Fallow field                                      | 14.7   | 5.1   | 2.4                     | 3.0   |
| Deciduous forest                                  | 58.9   | 20.6  | 5.2                     | 6.3   |
| Horticultural land                                | 15.4   | 5.4   | 1.1                     | 1.4   |
| Orchard   | 6.2  | 2.2   | 2.6                     | 3.2   |
| Forest plantation                                 | 22.5   | 7.9   | 6.6                     | 8.1   |
| Crop field  | 12.3   | 4.3   | 16.3                    | 19.9  |
| Urban village                                     | 15.1   | 5.3   | 5.1                     | 6.2   |
| Water   | 3.3  | 1.1   | 2.3                     | 2.8   |
| Range land  | 10.1   | 3.5   | 9.7                     | 11.8  |
| Paddy field                                       | 38.9   | 13.6  | 7.9                     | 9.7   |
| Barren land                                       | 3.9  | 1.4   | 5.8                     | 7.1   |
| Pasture   | 20.6   | 7.2   | 11.8                    | 14.4  |
| Wetland   | 32.7   | 11.4  | 3.6                     | 4.4   |
| Total   | 285.7  | 100.0 | 81.7                    | 100.0 |

were combined with the Landsat and PALSAR images (i.e. LPES-SC). An overall accuracy of 89.7 % was achieved with the Kappa coefficient of 0.88 (Table 1). A thematic land use/cover map was thus produced using the LPES-SC classification (Figure 4). The results show that deciduous forest is the dominant land cover class in the study area at 25.1%, followed by forest plantation at 15.9% and evergreen forest at 15.2% (Figure 4). Together, these three land use/cover classes accounted for more than 50% of the landscape. The three largest agricultural land use classes were crop field, fallow field, and orchard, accounting for 9.3%, 6.3%, and 4.7% of the study area, respectively. The accuracies for these forest and agricultural related land use/cover classes using the multi-sensor classification of LPES-SC were all above 80% (Table 1).

**Conclusions and future work**

The study assessed the potential of using multi-sensor data sets in land use/cover mapping in a tropical mountainous environment. The data sets used included the multi-temporal ALOS-PALSAR images, spectral features from Landsat TM, and topographic information of elevation

and slope. Multi-temporal PALSAR images were first used in short crop mapping of crop and paddy fields because radar images provided complementary information on agricultural land use during the rainy season. Accuracy assessments were next conducted to evaluate the classification results of 12 different combinations of the multi-sensor data sets. The results showed an increased overall accuracy from 19.2% using the PALSAR image alone to 87.7% with the LPES classification, and it improved to 89.7% when short crop mapping was further integrated with the LPES. Because of the mountainous terrain of the study area, elevation and slope played an important role in accounting for the distribution of land use/cover patterns. Incorporating terrain information was thus useful in improving the classification accuracies. In particular, elevation and slope data derived from a DEM provided valuable ancillary data, which was evident in the increased producer’s accuracy from 37.5% with P to 75% with PE for the evergreen forest class. Also, fallow field, deciduous forest, forest plantation, and paddy field all had relatively low accuracies when classifications were made using remote sensing images only, but adding elevation

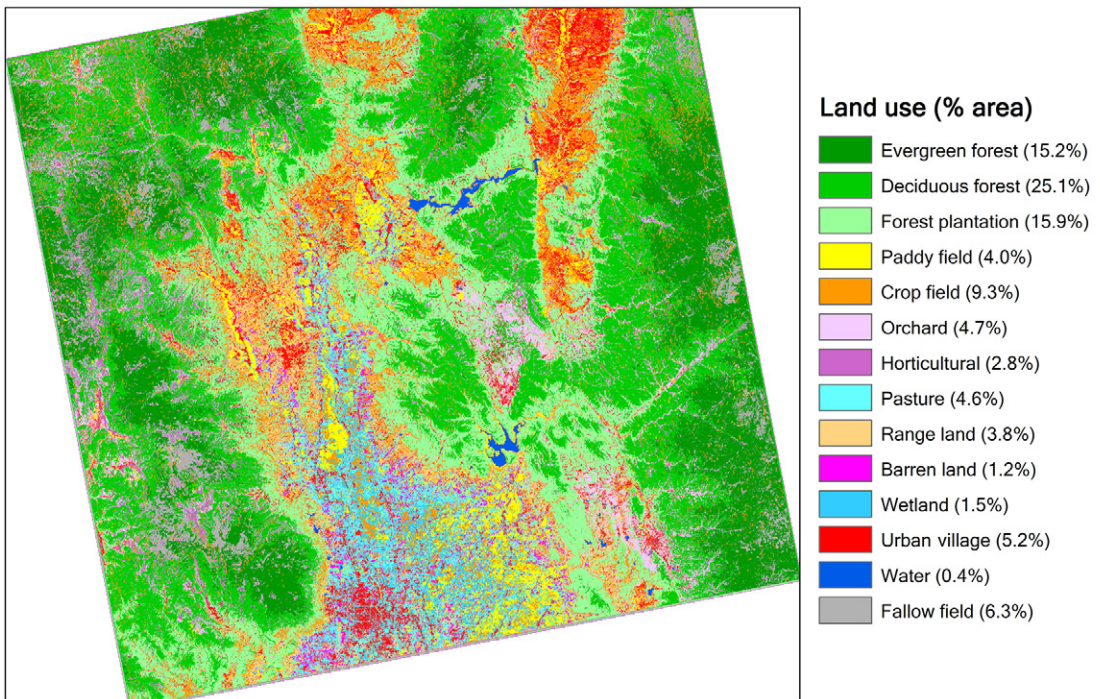


Figure 4 Land use/cover map produced using the multi-sensor classification of Landsat Thematic Mapper-Phased Array type L-band Synthetic Aperture Radar-elevation-slope-short crop.

and slope as input bands for classification greatly improved the accuracies.

The study presented a useful method for land use/cover mapping in mountainous areas where persistent cloud cover during the rainy season inhibited the use of optical images. The study used the MLC, a commonly used technique in the remote sensing literature. An alternative classifier, such as an artificial neural network (e.g. Sunar Erbek *et al.*, 2004; Lein, 2009), could also be useful because it requires no *a priori* knowledge about the statistical distribution of the input land use/cover class data.

#### ACKNOWLEDGEMENTS

The authors wish to thank the National University of Singapore for providing funding support through the research grant R-109-000-070-101 and the Faculty of Arts and Social Sciences Staff Research Support Scheme, Dr Wayne Stephenson and two anonymous reviewers for their comments, and Yikang Feng and Li-Kheng Lee for their assistance in mapping.

#### REFERENCES

- Achard, F., Eva, H.D., Stibig, H.J., Mayaux, P., Galleo, J., Richard, T. and Malingreau, J.P., 2002: Determination of deforestation rates of the world's humid tropical forests. *Science* 297, 999–1002.
- Anderson, J.R., Hardy, E.E., Roach, J.T. and Witmer, R.E., 1976: A land use and land cover classification system for use with remote sensor data. *U.S. Geological Survey Professional Paper No. 964*. U.S. Geological Survey, Washington D.C.
- Aschbacher, J., Ofren, R., Delsol, J.P., Suselo, T.B., Vibulsresth, S. and Charrapat, T., 1995: An integrated comparative approach to mangrove vegetation mapping using advanced remote sensing and GIS technologies: preliminary results. *Hydrobiologia* 295, 285–294.
- Asner, G.P., Rudel, T.K., Aide, T.M., Defries, R. and Emerson, R., 2009: A contemporary assessment of change in humid tropical forests. *Conservation Biology* 23, 1386–1395.
- Baraldi, A. and Parmiggiani, F., 1995: A refined gamma MAP SAR speckle filter with improved geometrical adaptivity. *IEEE Transactions on Geoscience and Remote Sensing* 33, 1245–1257.
- Bartalev, S.A., Belward, A.S., Erchov, D.V. and Isaev, A.S., 2003: A new SPOT4 vegetation derived land cover map of northern Eurasia. *International Journal of Remote Sensing* 24, 1977–1982.
- Earth Remote Sensing Data Analysis Center (ERSDAC), 2009a: ERSDAC PALSAR ortho product formats, revised R01.1. Retrieved: 1 June 2011 from [http://www.palsar.ersdac.or.jp/e/guide/pdf/PG-M-E-0188-R01\\_1\\_en.pdf](http://www.palsar.ersdac.or.jp/e/guide/pdf/PG-M-E-0188-R01_1_en.pdf)
- Earth Remote Sensing Data Analysis Center (ERSDAC), 2009b: ASTER global DEM validation summary report. Retrieved: 1 June 2011 from [http://www.ersdac.or.jp/GDEM/E/image/ASTERGDEM\\_ValidationSummary\\_Report\\_Ver1.pdf](http://www.ersdac.or.jp/GDEM/E/image/ASTERGDEM_ValidationSummary_Report_Ver1.pdf)
- Ekasingh, B., Ngamsomsuk, K., Letcher, R.A. and Spate, J., 2005: A data mining approach to simulating farmers' crop choices for integrated water resources management. *Journal of Environmental Management* 77, 315–325.
- Foley, J.A., DeFries, R., Asner, G.P., Barford, C., Bonan, G., Carpenter, S.R., Chapin, F.S., Coe, M.T., Daily, G.C., Gibbs, H.K., Helkowski, J.H., Holloway, T., Howard, E.A., Kucharik, C.J., Monfreda, C., Patz, J.A., Prentice, I.C., Ramankutty, N. and Snyder, P.K., 2005: Global consequences of land use. *Science* 309, 570–574.
- Gao, J., 2009: *Digital Analysis of Remotely Sensed Imagery*. McGraw-Hill, New York.
- Gardner, S., Sidisunthorn, P. and Anusarnsunthorn, V., 2007: *A Field Guide to Forest Trees of Northern Thailand*. Kobfai Publishing Project, Bangkok, Thailand.
- Giri, C., Defoumy, P. and Shrestha, S., 2003: Land cover characterization and mapping of continental Southeast Asia using multi-resolution satellite sensor data. *International Journal of Remote Sensing* 24, 4181–4196.
- Haack, B. and Bechdol, M., 2000: Integrating multisensor data and RADAR texture measures for land cover mapping. *Computers & Geosciences* 26, 411–421.
- Hamilton, S.K., Kellndorfer, J., Lehner, B. and Tobler, M., 2007: Remote sensing of floodplain geomorphology as a surrogate for biodiversity in a tropical river system (Madre de Dios, Peru). *Geomorphology* 89, 23–38.
- Ismail, M.H. and Jusoff, K., 2008: Satellite data classification accuracy assessment based from reference dataset. *International Journal of Computer and Information Engineering* 2, 386–392.
- Japan Aerospace Exploration Agency, 2007: ALOS user handbook, NDX-070015. Retrieved: 1 June 2011 from [http://www.eorc.jaxa.jp/ALOS/en/doc/alos\\_userhb\\_en.pdf](http://www.eorc.jaxa.jp/ALOS/en/doc/alos_userhb_en.pdf)
- Kanellopoulos, I. and Wilkinson, G.G., 1997: Strategies and best practices for neural network image classification. *International Journal of Remote Sensing* 18, 711–725.
- Lein, J.K., 2009: Implementing remote sensing strategies to support environmental compliance assessment: a neural network application. *Environmental Science & Policy* 12, 948–958.
- Lillesand, T.M. and Kiefer, R.W., 1999: *Remote Sensing and Image Interpretation*, 4th edn. Wiley, New York.
- Lung, T. and Schaab, G., 2010: A comparative assessment of land cover dynamics of three protected forest areas in tropical eastern Africa. *Environmental Monitoring and Assessment* 161, 531–548.
- Mather, P.M., 2004: *Computer Processing of Remotely Sensed Images*, 3rd edn. Wiley, New York.
- Mayaux, P., Holmgren, P., Achard, F., Eva, H., Stibig, H.J. and Branthomme, A., 2005: Tropical forest cover change in the 1990s and options for future monitoring. *Philosophical Transaction of the Royal Society* 360, 373–384.
- Office of Agricultural Economics, 2007: Agricultural land use statistics by regions and provinces of Thailand, Thai year 2549. Retrieved: 1 June 2011 from [http://www.oae.go.th/download/article/article\\_20090417181149.html](http://www.oae.go.th/download/article/article_20090417181149.html) (in Thai).
- Pan, X.-Z., Uchida, S., Liang, Y., Hirano, A. and Sun, B., 2010: Discriminating different landuse types by using multitemporal NDXI in a rice planting area. *International Journal of Remote Sensing* 31, 585–596.
- Peng, X., Wang, J. and Zhang, Q., 2005: Deriving terrain and textural information from stereo RADARSAT data for mountainous land cover mapping. *International Journal of Remote Sensing* 26, 5029–5049.
- Sunar Erbek, F., Ozkan, C. and Taberner, M., 2004: Comparison of maximum likelihood classification method with supervised artificial neural network algorithms for land use activities. *International Journal of Remote Sensing* 25, 1733–1748.

- Thai Meteorological Department, 2010: Climate of Thailand. Retrieved: 1 June 2011 from <http://www.tmd.go.th/en/archive/surfacetemperature.php>
- Thanapakpawin, P., Richey, J., Thomas, D., Rodda, S., Campbell, B. and Logsdon, M., 2006: Effects of land use change on the hydrologic regime of the Mae Chaem river basin, NW Thailand. *Journal of Hydrology* 334, 215–230.
- Thomas, D.E., 2006: *Participatory Watershed Management for the Ping River Basin, Final Project Report*. Office of Natural Resources and Environmental Policy & Planning, Ministry of Natural Resources & Environment, Bangkok, Thailand.
- Thomas, D.E., Preechapanya, P. and Saipothong, P., 2004: *Developing Science-Based Tools for Participatory Watershed Management in Montane Mainland Southeast Asia, Final Report to the Rockefeller Foundation*. International Centre for Research on Agroforestry, World Agroforestry Center, Chiang Mai, Thailand.
- Verbesselt, J., Hyndman, R., Newnham, G. and Culvenor, D., 2010: Detecting trend and seasonal changes in satellite image time series. *Remote Sensing of Environment* 114, 106–115.
- Zhou, X. and Wang, Y.-C., 2011: Dynamics of land surface temperature in response to land use/cover change. *Geographical Research* 49, 23–36.